Journal of Biomaterials Applications
http://jba.sagepub.com/

Development of a pre-vascularized 3D scaffold-hydrogel composite graft using an arterio-venous loop for tissue engineering applications

Subha N Rath, Andreas Arkudas, Christopher XF Lam, Radoslaw Olkowski, Elias Polykandroitis, Anna Chróscicka, Justus P Beier, Raymund E Horch, Dietmar W Hutmacher and Ulrich Kneser

J Biomater Appl 2012 27: 277 originally published online 16 June 2011
DOI: 10.1177/0885328211402243

The online version of this article can be found at:
http://jba.sagepub.com/content/27/3/277

Published by:
SAGE
http://www.sagepublications.com

Additional services and information for *Journal of Biomaterials Applications* can be found at:

Email Alerts: http://jba.sagepub.com/cgi/alerts

Subscriptions: http://jba.sagepub.com/subscriptions

Reprints: http://www.sagepub.com/journalsReprints.nav

Permissions: http://www.sagepub.com/journalsPermissions.nav

Citations: http://jba.sagepub.com/content/27/3/277.refs.html

>> Version of Record - Aug 23, 2012

OnlineFirst Version of Record - Jun 16, 2011

What is This?

Downloaded from jba.sagepub.com at UNIVERSITAETSBIBLIOTHEK on October 14, 2013

Article

JOURNAL OF
biomaterials
applications

Journal of Biomaterials Applications
27(3) 277–289
© The Author(s) 2011
Reprints and permissions:
sagepub.co.uk/journalsPermissions.nav
DOI: 10.1177/0885328211402243
jba.sagepub.com
SAGE

Development of a pre-vascularized 3D scaffold-hydrogel composite graft using an arterio-venous loop for tissue engineering applications

Subha N Rath[1,2], Andreas Arkudas[2], Christopher XF Lam[1], Radoslaw Olkowski[3], Elias Polykandroitis[2], Anna Chróścicka[3], Justus P Beier[2], Raymund E Horch[2], Dietmar W Hutmacher[4] and Ulrich Kneser[2]

Abstract

Hyaluronic acid (HA) and fibrin glue (FG) are effective hydrogels for tissue engineering applications as they support tissue in-growth, retain growth factors, and release them slowly with time. The scaffolds, in combination with a hydrogel, effectuate a successful graft. However, the survival of a graft entirely depends upon a functional vascular supply. Therefore, hydrogels must support the in-growing vasculature. To study and compare the vascular patterns, HA and FG hydrogel-containing PLDLLA-TCP-PCL scaffolds were implanted in the groin of male Lewis rats and supplied with a micro-surgically prepared arterio-venous (A-V) loop. The rats were perfused with a vascular contrast media after 4 and 8 weeks and sacrificed for further analysis. The specimens were scanned with micro-CT to find the vascular growth patterns. Corrosion casting of blood vessels followed by SEM demonstrated a high vascular density near the parent blood vessels. Histologically, HA and FG implanted animal groups showed significant angiogenetic activity, especially within the pores of the scaffold. However, formation of new blood vessels was more conspicuously observed at 4 weeks in FG than HA implants. Furthermore, by 8 weeks, the number and pattern of blood vessels were comparable between them. At this time, HA was still present indicating its slow degradation. The finding was confirmed by histomorphometric analysis. This experimental study demonstrates that HA containing composite scaffold systems permit stabile in-growth of blood vessels due to sustained degradation over 8 weeks. HA is a potential matrix for a tissue engineered composite graft.

Keywords

Arterio-venous loop model, fibrin gel, hyaluronic acid, angiogenesis, PLDLLA-TCP-PCL, microvascular CT scanning

Introduction

The supply of nutrients and oxygen is the most limiting factor for the survival of a graft in tissue engineering applications. Most of the cells cannot survive if they are located beyond 200–500 μm distance from a capillary.[1,2] The central core of an implant is most likely to be jeopardized without vascular development and depending on the size of the implant, needs weeks of time. A functional micro-vascular network of a graft is an integral component for cells to grow, differentiate, and function. Therefore, for tissue engineering applications, three-dimensional (3D) scaffolds supplied with cultured cells or growth factors necessitate a fast development of functional vascular supply.[3]

For the induction of vascularization from the host blood vessels, the cascade of events starts from endothelial (precursor) cell (EC) migration in response to

[1]Division of Bioengineering, National University of Singapore, Singapore
[2]Department of Plastic and Hand Surgery, University of Erlangen Medical Center, Erlangen, Germany
[3]Department of Biophysics and Human Physiology, Medical University of Warsaw, Warsaw, Poland
[4]Faculty of Engineering, Faculty of Science, Institute of Health and Biomedical Innovation, Queensland University of Technology, Brisbane, Australia

Corresponding author:
Ulrich Kneser, Department of Plastic and Hand Surgery, University of Erlangen Medical Centre, Krankenhausstrasse 12, 91054 Erlangen, Germany.
Email: Ulrich.kneser@uk-erlangen.de

angio-inductive growth factors, especially VEGF. Needless to say, a number of approaches have been attempted either with EC or VEGF *in vitro* for a vascularized graft though they usually require additional factors for vasculature development.[4] At present, most approaches to support or induce vascularization of engineered tissues are based on the so called 'extrinsic' mode of vascularization, which does not allow transfer of vascularized grafts to a distant site.[5] Therefore, from a practical point of view, an axially vascularized tissue is preferable, where a central core of vessels supply the graft from inside out in a centrifugal manner. Clinically they can be immediately vascularized upon transplantation to a defect site either as a pedicled graft or using microsurgical techniques similar to free flaps.

Recently, a number of methods have been advised for successful induction of axial vascularization: An arterio-venous (A-V) shunt loop, typically made by an anastomosis between an artery and a vein by microsurgical techniques with inter-positional artery or vein graft;[1,6] A-V bundle with distally ligated vessels, or flow-through configuration of intact vessels have been successfully applied. Though all of these techniques allow generation of new tissue and blood vessels, the shunt loops especially with a venous graft showed a greater potential for vascularized tissue formation.[7,8]

Different components of the 3D scaffolds affect its degradation and angioinductive potential.[9] A number of biomaterials such as synthetic polymers, bioceramics, and some natural substances have been evaluated for bone engineering applications.[10] Saturated polyhydroxy esters such as poly(L-lactide-co-D,L-lactide) (PLDLLA) have high mechanical strength, controllable degradation with metabolizable byproducts, and significant osteo-conductive potential.[11,12] Poly(ε-caprolactone) (PCL), another elastomeric polyester, can be used to enhance bone regeneration.[13] In combination, they effectuate an optimum scaffold, because PLDLLA degrades fast, while PCL degrades slowly. In addition to them, β-tri-calcium phosphate (TCP) is incorporated to provide hydrophilicity and counteract any pH alteration.[14]

Although the above-mentioned scaffolds provide mechanical support, they may not actively aid in cell integration and differentiation, because the synthetic polymer does not provide adequate chemical signals for transplanted or host-derived cells. To achieve this, ECM-components can be incorporated or other functional domains can be enriched on the surface.[15] An alternative technical approach, which mimics the physiological environment, is to use a biomimetic temporary cell carrier in the form of a hydrogel around the scaffold. A significant advantage of hydrogels compared to the relatively hydrophobic polymers is that cell receptor ligands and other molecules can be easily incorporated in them to achieve cell adhesion, migration, and differentiation.[16,17] They can also act as a temporary reservoir for growth factors and allow sustained and controlled release of these bioactive molecules over time.[18]

Fibrin glue (FG) is one of the commonly used hydrogel for such applications. It has been used for delivery of growth factors for wound healing, bone induction, and angioinduction in numerous tissue engineering applications.[1,19] Hyaluronic acid (HA) plays an important role in cell proliferation, morphogenesis, wound repair, and inflammation. In addition, HA oligosaccharides promote angiogenesis, while high molecular weight HA retards it.[20] A modified HA hydrogel is reported, which is a nonsulfated glycosaminoglycan, distributed widely in extracellular matrix.[21] Both hydrogels have promising properties that might allow generation of biologically active engineered tissues for different types of applications.

The aim of the present study was to develop a polymer-hydrogel composite that might be used for generation of axially vascularized bioartificial bone tissues. The biocompatibility of PLDLLA-TCP-PCL scaffolds to osteoblast-like cells was evaluated *in vitro*. The influence of two different hydrogel matrices (HA and FG) in composite porous polymer scaffolds on vascular ingrowth was investigated in an axial isolation chamber vascularization model and resorption kinetics of these matrices were assessed.

Materials and methods

Scaffolds

Scaffold fabrication. The scaffolds were fabricated using an in-house rapid prototyping (RP) system, namely the screw extrusion system (SES), utilizing three different materials: Poly(L-lactide-co-D,L-lactide) (PLDLLA, Boehringer-Ingelheim, Ingelheim am Rein, Germany), Poly(ε-caprolactone) (PCL, Absorbable Polymers, US), β-tri-calcium phosphate (TCP, Progentix, MB Bilthoven, Netherlands), in a ratio of 64%, 16%, and 20%, respectively by weight. The details of the fabrication method are described elsewhere.[22] Briefly, it exploits a layer-by-layer fabrication technique to assemble 3D structures by depositing two-dimensional (2D) supporting struts based on specified lay-down patterns to assemble the whole structure. Material is fed into the top of the barrel chamber, heated to a molten liquefied state at 120°C and transported towards a 400 μm nozzle with aided displacement and pressure from the turning screw feed.

Scaffold sheets of $50 \times 50 \times 1.5\,mm^3$ were fabricated with a 0°–90° lay-down pattern. Discs with 8 mm diameter were punched out from it and fabricated into

bobbin-shaped constructs using cylindrical pieces of 1.5 mm radius and 1.5 mm height for *in vivo* experiments using minimal amounts of chloroform (JT Baker, NJ, US), after which they were dried in a vacuum oven for 12 h (Figure 1(a)). The scaffolds were treated with 5 M sodium hydroxide for 5 min and rinsed with de-ionized water to yield a hydrophilic and corrugated surface. They were sterilized in 70% ethanol overnight followed by UV light for 2 h. Scaffold pieces of $5 \times 5 \times 8\,mm^3$ were cut for mechanical tests and porosity measurement.

Porosity and mechanical properties of the scaffolds. Scaffold porosity was measured as a ratio of true volume to apparent volume. The true volume (V_t) was determined by a gas pycnometer (Accupyc 1330, Micromeritics Instrument Corp., US) at 25°C in pure Helium. The apparent volume (V_a) is the geometrical volume. The porosity was confirmed by micro-CT (Skyscan1076, Kontich, Belgium) using 5 μm spot size at 100 kV with a resolution of 35 μm. Mechanical compression tests were conducted by a uniaxial material testing system with a 5-kN load cell, in accordance with ASTM D695-96 guidelines (Instron 3345, Grove city, PA, US). The scaffolds were compressed at a rate of 1 mm/min up to 0.6 strain level. They were tested both in dry and wet states ($n = 5$ for each). In wet state, they were soaked at 37°C in a water bath for 60 min prior to the testing. The stress–strain (σ–ε) curves were obtained to evaluate the compressive stiffness (modulus) and yield strength of the scaffolds. The stiffness was calculated from the σ–ε curve as the slope of the initial linear portion of the curve. The compressive yield strength was taken at the yield point (if any) or at the end of the linear region.

In vitro *evaluation*

Experimental design. Scaffold sheets of $50 \times 50 \times 3\,mm^3$ were fabricated with a 0°–90° lay-down pattern, from which scaffold pieces of $5 \times 5 \times 3\,mm^3$ were cut for *in vitro* cell culture

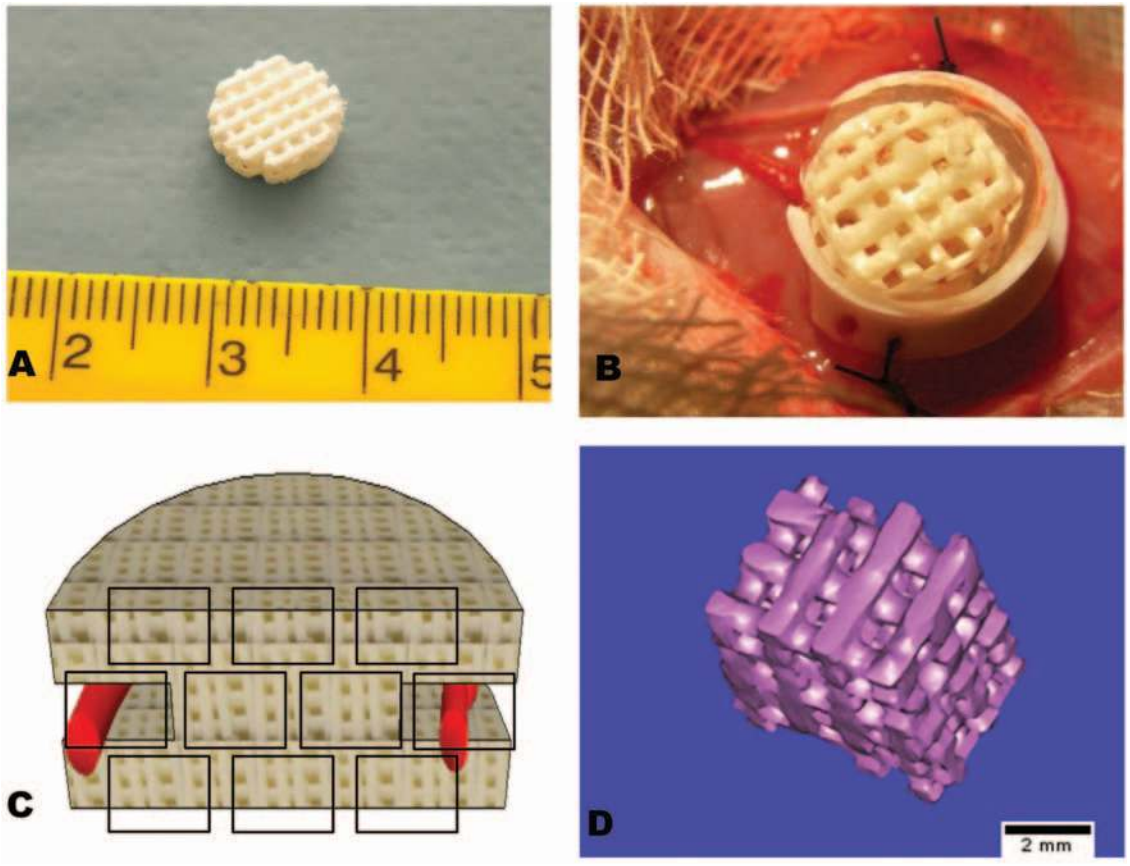

Figure 1. (a) Gross scaffold that was used for *in vivo* experiments shows uniform porosity. (b) An arteriovenous (A-V) loop was constructed from left femoral artery and vein using contralateral vein graft and placed surrounding the scaffold along with the hydrogel in a custom-made Teflon chamber. (c) Schematic representation of the scaffold for histomorphometric analysis. (d) The reconstructed image of micro-CT, used for *in vitro* tests, shows uniform porosity.

Table 1. Groups and study design.

In vitro group (n=)	Weeks after seeding	PicoGreen	BSA assay	SEM and confocal	*In vivo* group (n=)	Weeks after implantation	Histology and Histomorp hometry	Micro CT	Corrosion casting
9	1 week	6	6	0	A (10)	4 weeks	4	(2)	1
9	2 weeks	6	6	4		8 weeks	4	(2)	1
9	4 weeks	6	6	0	B(10)	4 weeks	4	(2)	1
9	6 weeks	6	6	4		8 weeks	4	(2)	1

In vitro tests are performed with 12–16 scaffolds per time with four different time points, week 1, 2, 4, and 6. For *in vivo* experiments, in group A animals, an arteriovenous (AV) loop was constructed and put around the scaffold with fibrin glue matrix. In group B, the same procedure was followed with a hyaluronan-based hydrogel. Two out of the five samples *in vivo* samples used for micro CT examinations.

experiments. The experimental setup was divided into 4 time points (1 week, 2 weeks, 4 weeks, or 6 weeks) and was documented in (Table 1).

Biocompatibility with osteoblasts. To analyze the biocompatibility of the scaffold materials *per se*, an osteoblast-like human osteosarcoma cell line (MG-63, ATCC, Manassas, VA, US) was used. The cells were cultured using expansion media (DMEM with 10% Foetal Bovine Serum, 1% Penicillin-Streptomycin, and 2 mM L-glutamine - all from Gibco, Invitrogen, CA, US). Each scaffold was seeded with 300,000 cells. The cell-scaffold constructs were further cultured in differentiation media with 25 mM HEPES (Gibco, Invitrogen, CA, US), 10 mM beta-glycerophosphate, 100 µm L-ascorbic acid-2-phosphate, and 10 nM dexamethasone (all from: Sigma, St. Louis, MO, USA). The culture was maintained until 6 weeks at 37°C and 5% CO_2 with twice weekly media change. The cell-seeded scaffolds were observed by an inverted microscope (Nikon Eclipse TE2000-U, Kanagawa, Japan).

To analyze the cell proliferation and the protein content, cell-seeded scaffolds were washed with 1x PBS and then treated by lysis buffer containing 0.1% Triton-X in 10 mM Tris-HCl buffer (Sigma, St. Louis, MO, USA). The lysates were frozen at -80°C and later analyzed. Cell proliferation was evaluated using PicoGreen DNA quantification assay (Molecular Probes Inc., Eugene, US) as advised by the manufacturer. The fluorescence was measured at excitation and emission wavelength of 485 and 520 nm respectively by a fluorescent microplate reader (Fluostar Optima, BMG Labtech, Germany). The values are converted to DNA amounts in ng/mL, corrected with blanks. The total protein content was assessed by BCA Protein Assay Kit (Pierce Biotechnology, Rockford, IL, USA), as advised by the manufacturer.

To visualize the viable and nonviable osteoblasts, cell-seeded scaffolds were washed with 1×PBS and incubated with 2 µg/mL fluorescein diacetate (FDA) (Molecular Probes Inc., Eugene, US) at 37°C for 15 min. They were rinsed twice in 1×PBS and placed in 20 µg/mL propidium iodide (PI) solution (Invitrogen, CA, US) at room temperature for 2 min. Subsequently, they were viewed under a confocal laser scanning microscope (Nikon Eclipse TE2000-E, Kanagawa, Japan). The viable-cell cytoplasm was labeled green, while nonviable cell nuclei were labeled red. Additional cell-seeded scaffolds were fixed in 2.5% glutaraldehyde (Carl Roth GmBH, Germany) in cacodylate buffer (Sigma, St. Louis, MO, USA) and dehydrated in a gradient ethanol series up to 100% and left to dry at room temperature. They were then observed by a scanning electron microscope (Hitachi TM 1000, Tokyo, Japan).

In vivo *evaluation*

Experimental design. With approval by the animal care committee of the University of Erlangen and the government of Mittelfranken, Germany, 20 inbred male Lewis rats (Charles-River, Sulzfeld, Germany) weighing 200–300 g were used. Animals were kept in 12 h dark–light cycle with free access to standard chow (Altromin, Hamburg, Germany) and water at the veterinary care facility of the University of Erlangen Medical Center.

The rats were divided into two groups, each consisting of 10 animals. The PLDLLA-TCP-PCL scaffold was loaded with either 1 mL of FG (group A) or 1 mL of hyaluronan-based hydrogel (group B) prior to implantation. In group A, a clinically approved fibrin gel (Tissuecol, Baxter, Vienna, Austria) was used with 1:1 mixture of fibrinogen (20 mg/mL in aprotinin) and thrombin (4 IU/mL in 40 mM calcium chloride). The hyaluronan-based (HA) hydrogel (Extracel-HP, Glycosan BioSystems, Salt Lake City, Utah) was supplied as a kit consisting of three components, namely thiol-modified hyaluronan and heparin, thiol-modified gelatine, and thiol-modified cross-linker,

polyethylene glycol diacrylate. The components were prepared with distilled water at 37°C under aseptic conditions and were mixed at 2:2:1 ratio, respectively, according to the manufacturer's recommendations. After all components were thoroughly mixed, the hydrogels were added as such to the AV loop-scaffold constructs. The hydrogels were less viscous to fill up the void space homogeneously before *in situ* polymerization set in few minutes to make a gel-like composition.

Surgical procedure and explantation

All surgical procedures were performed by experienced microsurgeons using a surgical microscope (Karl Zeiss, Jena, Germany) under general anaesthesia with Isoflurane (Baxter, Unterschleißheim, Germany). The surgical technique has been described previously by our group.[23] In brief, the femoral vessels were exposed by a longitudinal incision from the inguinal ligament to the knee. The sheath of the neurovascular bundle was opened. After exposure of the right-sided femoral vessels, a 20 mm vein graft was harvested from the right femoral vein. An A-V loop was created by interposition of the vein graft between the left sided femoral artery and the left femoral vein with interrupted non-absorbable 11-0 nylon stitches (Ethilon, Ethicon GmbH, Norderstedt, Germany). The A-V loop was placed around the PLDLLA-TCP-PCL scaffold and submerged in the hydrogel as per the groups (Figure 1(b)). The whole construct was placed in a sterile cylindrical teflon-chamber (inner diameter 10 mm, height 6 mm, constructed by the Institute of Materials Research, Division of Glass and Ceramics, University of Erlangen). The chamber was then capped and fixed to the underlying muscle. The skin was closed using interrupted 3-0 vicryl sutures (Ethicon GmbH, Norderstedt, Germany). All animals received 0.2 mL benzylpenicillinbenzathine (Tardomycel; Bayer, Leverkusen, Germany), buprenorphine (0.3 mg/kg rat weight) (Temgesic; Essex Chemie AG, Luzern, Switzerland), and heparin (80 IU/kg) (Liquemin; Ratiopharm, Ulm, Germany) postoperatively.

Explantation of the specimens was performed after 4 and 8 weeks. The aorta was cannulated and the vascular system was rinsed with heparinized Ringer solution (100 IU/mL) under hydrostatic pressure, until fluid escaping from the severed inferior vena cava was clear. One specimen from each group was used for corrosion casting as described later. The other rats were perfused with a vascular contrast media, Microfil (MV-122, Flowtech, Mass., USA) under general anesthesia for micro-CT analysis. The distal vascular system was then injected with 20 mL of Microfil containing 5% of MV Curing Agent as advised by the manufacturer. Finally the aorta and caval vein were ligated and the rats were cooled at 4°C for 24 h. Specimens were explanted *in toto* and fixed in 3.5% formalin.

Micro-CT analysis

For each experimental group, two specimens were randomly selected. They were scanned on a high resolution 'ForBild' scanner developed by Institute of Medical Physics, FAU Erlangen-Nuremberg, Germany. The constructs were scanned with following parameters: Al-0.5 mm filter, tube voltage of 40 kV, 15 μm pixel size, and 15 μm slice distance between consecutive slices. The data were volumetrically re-constructed using ImpactView software (Vamp GmbH, Erlangen, Germany) in a 1024*1024 pixel matrix.

Corrosion cast technique

The vascular corrosion casts were prepared for visualization of detailed microstructure by scanning electron microscope (SEM) as described elsewhere.[24] Briefly, the vascular system of the rat was rinsed with heparinized Ringer solution and was then rinsed with 10 mL of half-strength Karnovsky solution (0.25% glutaraldehyde, 0.25% paraformaldehyde, and 0.1 M Na-cacodylate buffer adjusted to a pH of 7.2). The vascular system was then perfused with 20 mL of methylmethacrylate (MMA) resin in a mixture of 4:1 pre-polymerized oligomer to MMA monomer (Sigma Aldrich Chemie GmbH, Munich, Germany) and benzoyl oxide as a catalyst (Mercox; Ladd Research Industries, Burlington, Vt.). The rat was left in a warm water bath (50°C) for 6 h to form the poly-MMA vascular replica after complete polymerization. The construct was then left for 12 h in 7.5% sodium hydroxide at 60°C. The cycle was repeated three times. The sample was decalcified by keeping it in 2.5% hydrochloric acid at room temperature for 12 h. The vascular replicas were finally dried by lyophilization before observing under a SEM (Quanta 200, FEI Company, Hillsboro, USA).

Histology and histomorphometry

The samples were serially dehydrated and paraffin embedded according to standard protocols. Five **micron** sections were taken using a microtome (Leica RM 2135, Wetzlar, Germany). All the slides were stained with Hematoxylin and eosin (H & E) using a fully automated process (Jung Auto Stainer XL, Leica Microsystems, Nussloch, Germany). Immunhistochemical analysis was performed using rabbit polyclonal antibodies against vWF (von-willebrand factor) (A0082, Dakocytomation, Carpinteria, CA, USA) at 1:500 dilution to confirm the vascular endothelium.

Envision HRP anti-rabbit kit (K4011, Dakocytomation, Carpinteria, CA, USA) was used as secondary antibody.

The histomorphometric analysis was performed by two blinded, independent observers as described elsewhere.[25] Briefly, the images of two standardized planes (500 μm proximal and 500 μm distal to the central plane) were photographed and oriented perpendicular to the longitudinal axis of A-V loops. All images were taken by a light microscope with bright-field filter (Leica DM IRB, Wetzlar, Germany). The images of each cross section were set together and rendered bimodal (ImageJ, NIH, Maryland, US). The construct size (cross-sectional area) and the area of fibro-vascular tissue (FVT) were measured for each of the sections. The number of blood vessels was counted as the Microfil-filled vessels in 10 pre-selected fields of view (four in the central region and three each in upper and lower parts of the construct) at 100× magnification (Figure 1(c)). Results are expressed as means ± standard errors of the mean.

Statistical analysis

All *in vitro* results were statistically compared by Kruskal–Wallis nonparametric ANOVA test followed by *post hoc* Dunn's test (GraphPad InStat, La Jolla, CA, USA). The results were expressed as means ± standard deviation. For histomorphometric analysis, two-way ANOVA test was performed followed by Bonferroni's post-test and standard error bars were included. For all pair-wise comparisons on quantitative results, Student's *t*-test was used. The results were considered significant at $p < 0.05$.

Results

Scaffolds

Gross morphology and porosity. Grossly, PLDLLA-TCP-PCL scaffolds have highly porous 3D structure with uniformly arranged individual layers of struts at 0° and 90° angles (Figure 1(a)). Visual observation and micro-CT reconstructed images demonstrate the homogeneity and consistency of the deposited struts (Figure 1(a) and (d)). The pores are also regular and coherent. In micro-CT analysis, the scaffolds show a regular spatial arrangement of pores, which are fully interconnected. The scaffolds exhibit porosity of 57–63% and pore sizes of 600–900 μm in the *x–y* plane and 200–300 μm in the *z*-axis.

Mechanical properties

The composite scaffolds exhibited a compressive stiffness of 209.06 ± 16.86 MPa and a yield stress (strength) of 7.29 ± 0.69 MPa in dry state. In wet state, the stiffness was about 138.07 ± 16.47 MPa, while the yield strength was about 8.31 ± 2.08 MPa. Though, the changes in stiffness are significantly different, the yield stress changes are not different at $p < 0.05$ level.

In vitro *evaluation*

Microscopic observation. After 2 weeks of *in vitro* culture, the struts of scaffolds were colonized with numerous cells forming a cell sheet in SEM and light microscope. After 6 weeks, the cells and the extracellular matrix form a dense sheet, which covers the struts and fills the pores of the scaffold. Vitality of the cells was demonstrated over the entire observation period by FDA/PI staining (Figure 2).

Biocompatibility assays. The dsDNA values of the cell-seeded scaffolds increased progressively until week 4 followed by a slow decline by week 6. The amount of deposited protein in these constructs is progressively increased to culminate by 6th week (Figure 3).

In vivo *evaluation*

All animals tolerated the surgical procedure well without any major postoperative complications. Grossly, animals with patent loops showed two major Microfil-filled blood vessels running into the chamber, which was later confirmed by histology and micro-CT. The two specimens with nonpatent A-V loops, one each from 4-week Group A and 8-week group B, were excluded from further analysis.

Micro-CT analysis and corrosion casting

The pattern and distribution of angiogenesis of representative samples in micro CT scanning were shown for scaffolds with either fibrin gel (group A) or hyaluronan hydrogel (group B) (Figure 4(a)–(d)). In FG, the number of blood vessels was maximum at 4 weeks, which decreased nonsignificantly by 8 weeks. The blood vessels appeared to start sprouting from the A-V loop and to extend to the centre of the scaffold with time. By 8 weeks there was greater penetration of the scaffolds. Additionally, their branching vessels were increased by 8 weeks (Figure 4(a) and (b)).

On the contrary, in hyaluronan hydrogel, the newly grown vessels were obviously shorter at 4 weeks with branches only along the vascular axis without deeper penetration into the matrix. By 8 weeks, the sprouting

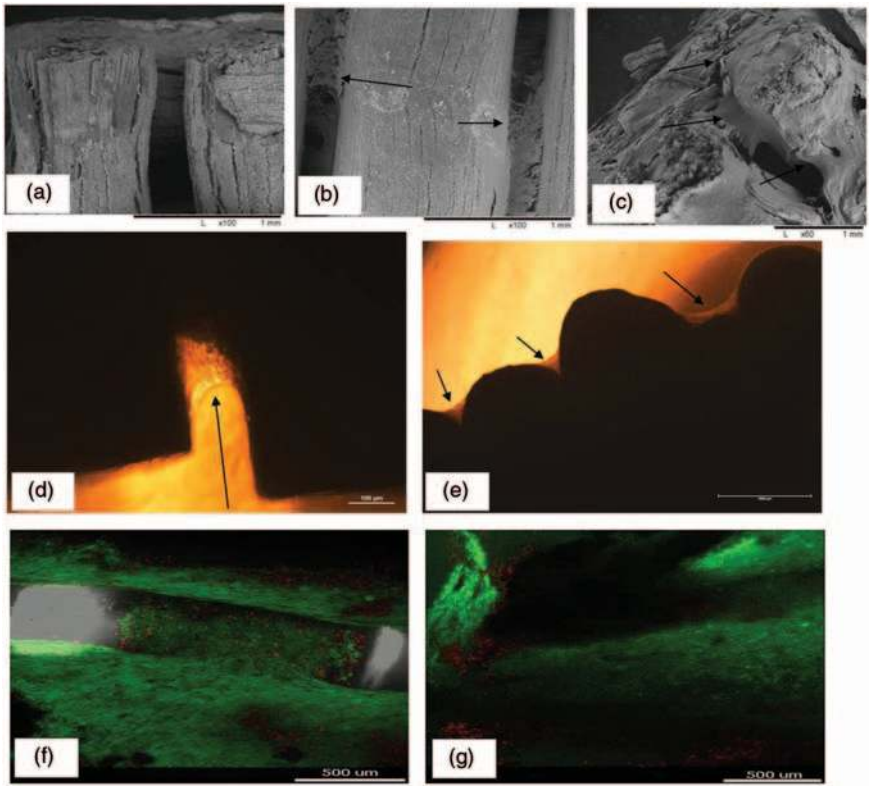

Figure 2. Microscopic images of *in vitro* cell-scaffold constructs. SEM pictures of PLDLLA-TCP-PCL scaffolds: (a) unseeded scaffold after 2 weeks of incubation in culture medium, (b) cell-seeded scaffold after 2 weeks, and (c) 6 weeks of culture in vitro. Arrows indicate the cell-ECM sheet on scaffold surface. Cell seeded PLDLLA-TCP-PCL scaffolds were observed in phase contrast light microscope after (d) 2 weeks and (e) 6 weeks in culture. Similar scaffolds in confocal microscope after (f) 2 weeks and (g) 6 weeks of culture. Living cells stained green and dead cells stained red.

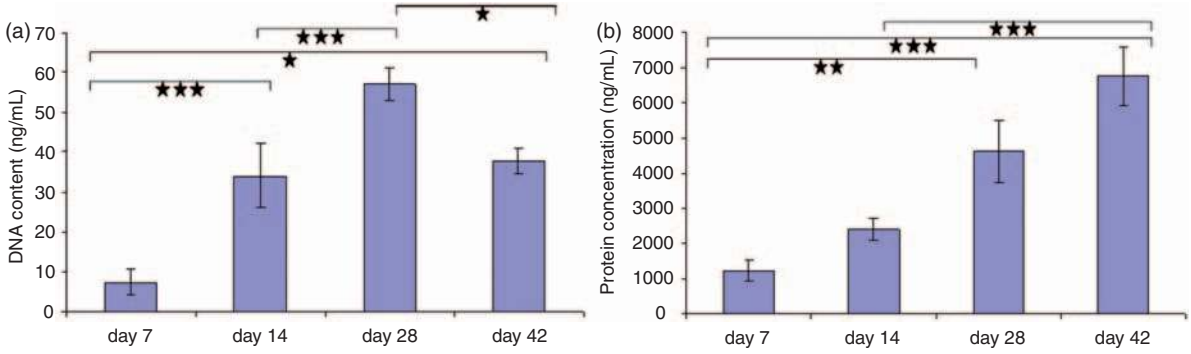

Figure 3. *In vitro* tests of PLDLLA-TCP-PCL scaffolds: (a) PicoGreen and (b) BCA assay. The difference is significant at $^{***}p < 0.001$, $^{**}p < 0.01$, $^{*}p < 0.05$.

blood vessels were clearly evident with elongated branches and deeper penetration into the matrix. In addition, by 8 weeks the vascular pattern was morphologically similar to that in FG matrix (Figure 4(c) and (d)).

The SEM images of corrosion cast replica of the vascular networks showed the detailed architecture inside the graft. At 4 weeks, angiogenetic sprouts appeared as spikes owing to increased permeability of the neo-capillary tip (Figure 4(e)). At 8 weeks of angiomorphogenesis, the neo-vascular network displayed a clear hierarchical arrangement of vessels in different orders (Figure 4(f)), from arterioles to pre-capillary arterioles and gas exchanging capillaries (CL),

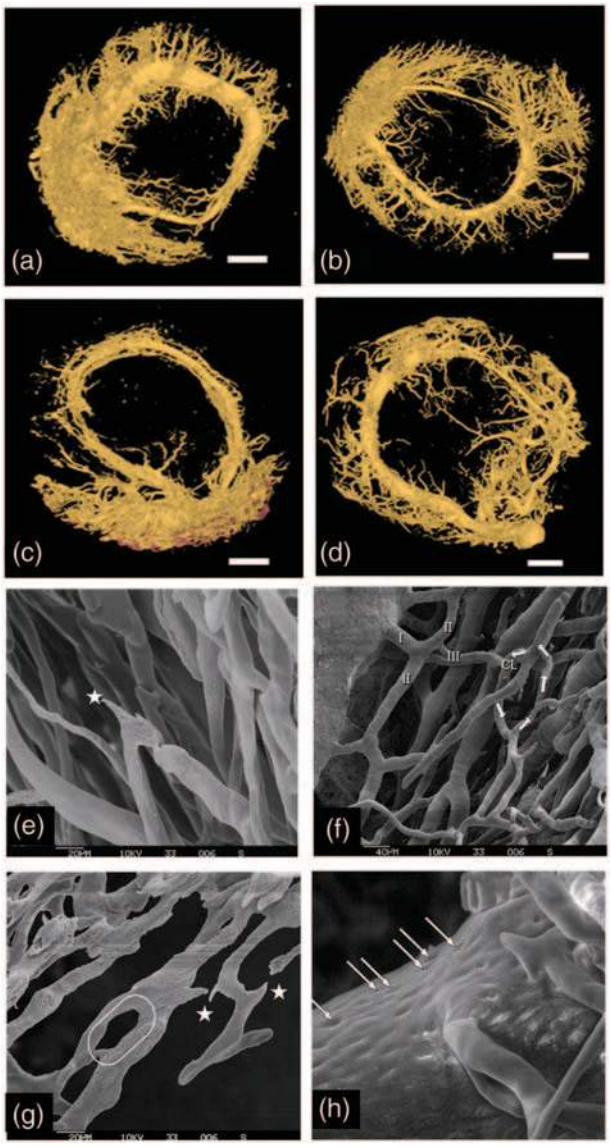

Figure 4. Micro CT images (a–d) of the Microfil infused constructs and SEM images (e–h) of vascular corrosion cast constructs. (a) A rich vascular network was observed at 4 weeks in fibrin glue constructs, which was stabile over time (b). In contrast, in hyaluronan matrix constructs a lower vascular density was observed at 4 weeks (c), which considerably increased until 8 weeks (d). Scale bars in (a-d) represent 2 mm. In SEM images, fibrin glue scaffolds after 8 weeks show angiogenic sprouts appearing as spikes (500×, asterisk) (e) and capillary loop formation (arrows) (f) were observed. The variability in caliber of vessels within one field as signs of vascular network maturity (250×) (g) and the pattern of nuclear imprints on microvascular replica at higher magnification (1200×) (h) were also observed. Similar observations were observed for hyaluronan scaffolds.

post-capillary venules draining into venules and veins. At sites of high angiogenetic activity, both intussusceptive (circle) and sprouting (asterisk) angiogenesis were observed (Figure 4(g)). The neo-capillary lumina were irregular and noncircular, but their calibers showed uniform sizes between 7 and 15 μm. The confirmatory identity of vessels was depicted at higher magnification by the pattern of the imprints of EC nuclei on microvascular replica (arrows) (Figure 4(h)). ECs covering the wall of the artery were appeared spindle shaped owing to the pulsatile shear stress, whereas the pattern on the veins was more rounded and dispersed.

Histology and histomorphometry

Histological photographs showed numerous Microfil-filled blood vessels (black) in specimens from all groups. A dense network of newly formed blood vessels originated from the A-V loop and progressively invaded the void spaces within the scaffolds in both groups. The cross-sectional photographs showed numerically higher number of vessels in pores near the vascular axis. There was no significant foreign body reaction detectable in those specimens. The scaffolds were not degraded *in vivo* in 8 weeks, but the sections presented them as blank areas, as they were dissolved during histological preparations. As expected, there was no specific tissue formation such as bone, adipose tissue in all sections; rather, a steady increase of FVT was evident over time. A representative figure of each type of sample was shown (Figure 5(a)–(d)). Immunostaining by vWF antibody demonstrated patency and functional integrity of blood vessels, positive with Microfil-filled (black) lumen (Figure 5(e) and (f)).

In histomorphometric analysis, in group A, the number of blood vessels per cross-section area were 104 ± 14.52 and 79.8 ± 11.25 for 4 and 8 weeks, respectively and the values for group B were 74.25 ± 12.58 and 67.33 ± 14.52 for 4 and 8 weeks, respectively. However, the values were not significantly different (Figure 6(a)).

The percentage of fibro vascular tissue (% FVT) was calculated by the ratio of total FVT area to total cross sectional area. For group A matrix, the % FVT values were 20.89 ± 1.42 and 23.67 ± 1.10 at week-4 and week-8 respectively, while for group B matrix, the corresponding values were 8.61 ± 1.23 and 16.28 ± 1.42 (Figure 6(b)). The group B values were significantly less ($p < 0.001$) in both time points than the group A values. However, the increment of FVT between the time points was significant only in group B (hyaluronan) matrices ($p < 0.001$). The numbers of blood vessels per mm^2 of FVT area for group A matrix were 11.09 ± 2.57 and 9.62 ± 1.99 at 4 weeks and 8 weeks respectively; while for group B matrix, the corresponding values were 19.49 ± 2.23 and 10.38 ± 2.57, respectively (Figure 6(c)**)**. At 4 weeks, the group B value was

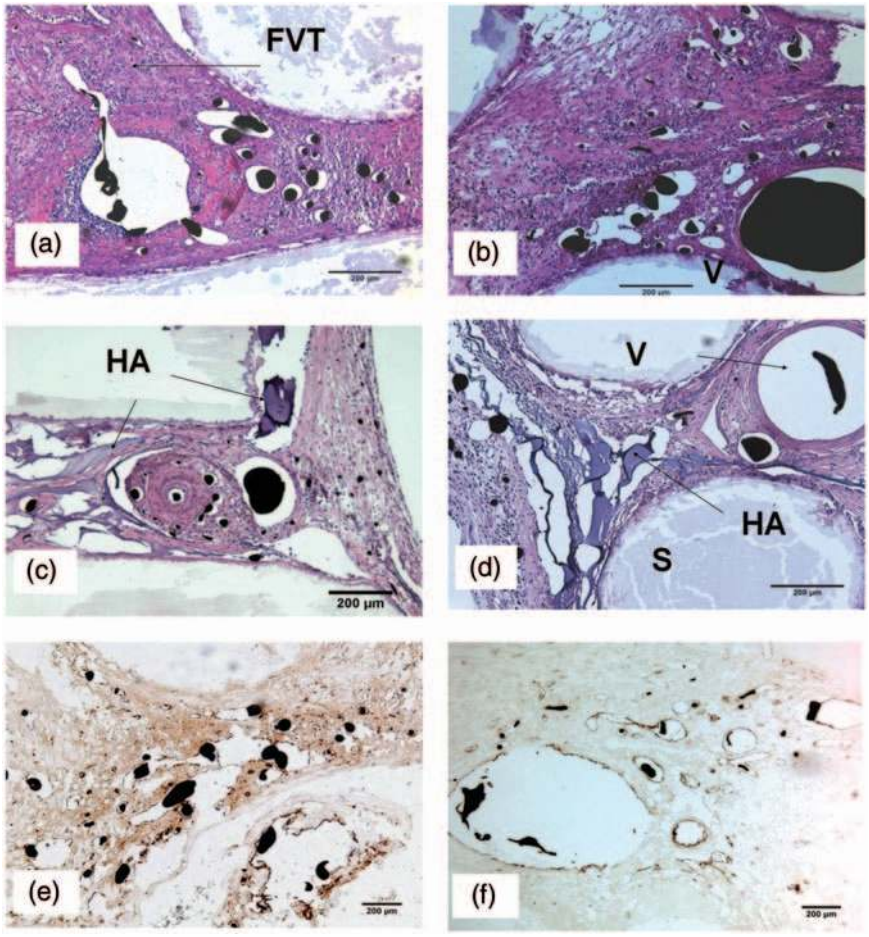

Figure 5. Hematoxylin and eosin staining of 100× magnified specimen of group A (a,b) and B (c,d) after 4 (a & c) and 8 (b & d) weeks. S: scaffold; HA: hyaluronic acid matrix; B: Microfil filled blood vessels; FVT: fibro vascular tissue; V: vein of the loop. Scale bar showing 2001m in all the figures. VWF (von Willebrand factor) immuno staining for fibrin glue (e) and hyaluronan (f) specimens after 8 weeks of implantation. The dark colored Microfil-filled vessels are simultaneously positive for VWF immunostaining (stained brown).

significantly higher than the group A value. Though there was no observed FG matrix in histological slides, the mean percentage of remaining hyaluronan hydrogel at week4 and week8 were 17.13 ± 3.05 and 13.62 ± 2.05 (Figure 6(d)), respectively. However, the two values are not significantly different.

Discussion

We have shown that PLDLLA-TCP-PCL, a composite polymeric scaffold, is biocompatible with osteoblast-like cells. The cells with the scaffold not only multiply but also produce proteins and extracellular matrix for a harmonious growth. Furthermore, the scaffold en bloc in presence of different hydrogels *in vivo* can function as a vascularized graft. To accomplish this, we have introduced two different hydrogels such as fibrin gel and hyaluronan around the scaffold, along with an A-V loop that makes the scaffold bio-integrated with the *in vivo* vascular system eventually producing a highly vascularized graft even without any growth factors in an ectopic site. The whole construct can be attractive, especially to create surgically implantable bone tissue engineered grafts.

A major drawback of using a pure biomaterial is that it can never mimic the complex nature of any tissue, especially bone. Therefore, a composite of polymer and ceramic is fabricated in this study by SES to avail the suitable properties of each of them. The mechanical properties of the scaffold are in the range of normal cancellous bone that has stiffness of 90–400 MPa and strength of 2–5 MPa.[26] Water makes the polymer chains plasticized and the embedded ceramic particulates solubilized, which could result in weakening of the reinforcement effect in wet conditions.[27] Along with highly interconnected pores, a typical porosity of 60–80% and pore diameter of at least 200 µm are known to be crucial to support vascularization and tissue in-growth.[28] The scaffolds have similar porous structure.

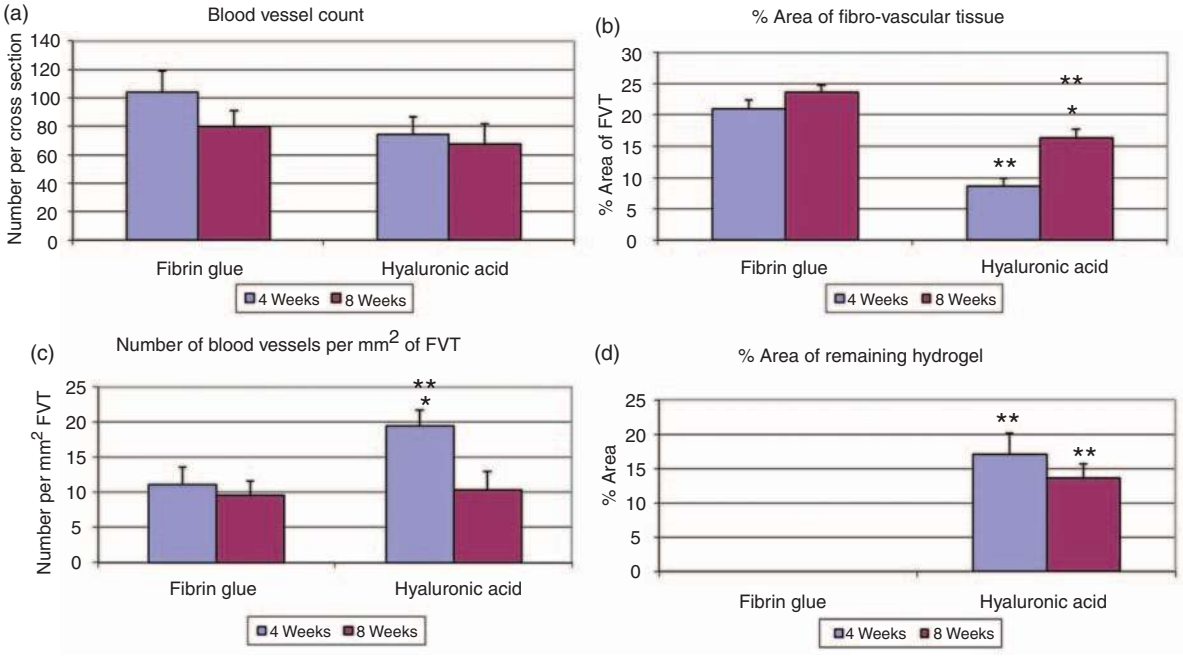

Figure 6. Histomorphometric calculations of blood vessel formation: (a) mean number of blood vessels per cross section in group A (fibrin glue only) and group B (hyaluronan matrix) specimens. (b) Mean percentage of FVT in each cross section in fibrin glue and hyaluronan matrices. (c) Mean number of blood vessels per mm^2 area of FVT per cross section. (d) Mean percentage of remaining hydrogel. Each experiment has $n = 3$ or 4; the values are in means $\pm$ SEM. The * indicates the significance between time points with same matrix and the ** indicates the significance between the matrices, at $p < 0.05$ levels.

The scaffold *per se* demonstrated *in vitro* growth compatibility with the osteoblast-like cells and supported their replication, as observed in light microscopic pictures and corroborated by PicoGreen assay until week 3 (Figures 2 and 3(a)). Thereafter, the minimal decline in PicoGreen assay might be due to maturation phase of cell growth cycle. However, the total amount of deposited protein is increasing continuously during the observation period (Figure 3(b)), which might be related to the formation of extracellular matrix. Confocal and SEM microscopic pictures show the osteoblast-like cells grow well on its surface with complete colonization and producing abundant extracellular matrix. Most of the cells are healthy and alive at all time points as seen by FDA/PI staining in confocal microscope (Figure 2(f) and (g)).

The composite scaffolds were successfully vascularized as demonstrated by micro-CT and histological analysis. In micro-CT angiograms, group A specimens displayed similar numbers of new blood vessels between 4 and 8 weeks. However, in group B, the observed number of blood vessels at 8 weeks was comparatively more than that at 4 weeks. Even so, by 8 weeks both the hydrogels showed a similar picture (Figure 4(a)–(d)).

In the histomorphometric analysis, though the numbers of vessels among different groups are not significantly different, the number of vessels per mm^2 of FVT is significantly higher in group B (hyaluronan) than that in group A FG at 4 weeks (Figure 6(c)); the difference is alleviated at 8 weeks. This indicates sprouting vessels are tightly packed in a smaller volume of FVT in group B at 4 weeks. By 8 weeks, however, vessels are evenly spaced with temporal degradation of hyaluronan. Interestingly, in group B between the two time points, the FVT area and the number of vessels per mm^2 of FVT were reciprocally different (Figure 6). This might be explained by the decreasing amount of remaining hyaluronan matrix at 8 weeks. The data correlated well with histological cross-sections.

In this experiment, two different kinetics of hydrogel degradation are highlighted, which have been shown to influence the type and generation of ECM.[29] The degradation allows migrating cells to produce ECM to replace the hydrogel. The byproducts may stimulate angiogenesis subsequently. FG is degraded *in vivo* primarily through cell-mediated serine-protease plasmin, which is competitively inhibited by a peptide, aprotinin. However, even with its presence, the constructs are typically resorbed within 5–10 days, when the aprotinin is not specifically bound by covalent linkage.[30] In FG specimens, there was a quick resorption of the matrix and the maximum uniform formation of blood vessels, starting from the beginning, which does not change subsequently. On the contrary, the modified hyaluronan is degraded slowly by hyaluronidase of the cells. Therefore the degradation promotes both cell mobility

and proliferation while supporting tissue morphology in an equivalent pattern.[31]

The findings have significant practical implications. The formation of invading differentiating functional tissues can be guided by the rate of degradation of hydrogel.[32] The quick fibrinolysis and the rapid angiogenesis are helpful for a quick generation of FVT in FG matrix. This graft, when seeded with tissue-specific cells or angio-inducing factors, is useful as a pre-vascularized graft.[1] However, with the quick release of its contained growth factors,[33] the fast degrading hydrogels like FG may not be effective directly for bone healing. When it degrades rapidly, the empty space is usually filled by fibrotic tissue without any properly differentiated tissue. A clear example was shown that faster degrading hydrogel do not synchronize with natural healing rate in a bone defect which typically requires 4–5 weeks.[32] Slowly degrading matrices achieve better bone healing, because continuous supply of osteogenic signals are assured.[34] In such cases, Hyaluronan hydrogel might be helpful. It may help for slow and sustained delivery of active biological cues that is an important benchmark for a mature tissue development. However, such speculations need to be properly investigated.

Riley et al. had shown the potential neo-vascularization ability of HA, which not only contained the growth factors by covalent bonding, but also released them slowly *in vitro* for 4–6 weeks.[35] However, few shortcomings are encountered for the application of the hydrogel, especially with a composite scaffold in the A-V loop chamber model. First, this activity was shown in ear pinnae of mice, where the vessels can grow randomly from anywhere around it as extrinsic vascularization. On the contrary, A-V loop model shows the axial vascularization and predicts precisely and quantitatively the inherent angioinductive nature of the hydrogel, avoiding random interference from the variable number of vessels present around. Secondly, they had shown the *in vivo* effect for 4 mm discs for a few weeks. However, HA is used for its longer stability *in vivo*. In many instances, the use of a hydrogel along with a hard scaffold is one integral component of a suitable graft. Therefore, our study necessitates the addition of PLDLA-TCP-PCL composite scaffold in wider dimensions for 4–8 weeks. Thirdly, we used a standardized protocol for counting the vessels after Microfil perfusion. The assessment of micro-vessel number might be erroneous and difficult to comment just from histology without injection techniques or specific immunostainins.[35]

The A-V loop model in an isolation chamber setting has not only experimental but also therapeutic implications. Currently, it offers opportunities to study 3D vessel in-growth into matrices of different origin and its modulation by either pro-angiogenic or anti-angiogenic agents. By appropriate alterations of the conditions around the A-V loop, one may also be able to create a standardized, isolated environment to study matrix behavior and angiogenetic phenomena.[3] Furthermore, the consequence of additional growth factors or cells on angiogenesis can also be precisely examined. In plastic surgery, the conventional prefabricated osteomyocutaneous flaps do not always meet the requirements of a composite defect. Therefore, utilizing patient's body as a bioreactor, a composite flap can be created as per the defect to meet such demand.[5] The tissue component can be fed by an A-V loop for microsurgical transfer after its complete development.[36]

The current study describes a composite pre-vascularized scaffold for tissue engineering application with continuous degradation and in-growth of vessels over time. Surgical free graft transfer with micro-vascular anastomosis is in practice for a long time in regenerative medicine to repair the diseased or damaged site with a healthy graft tissue, limited only by the availability of autograft. Our method is to create the donor graft, engineered to possess the complete functional vascular network to enable them as an ideal tissue engineered graft. In this study, a graft was prevascularized at different rates to the full extent with parental blood vessels.

Conclusions

In this study, we demonstrated that the SES system fabricated PLDLLA-TCP-PCL scaffolds possess suitable mechanical properties and are well compatible with osteoblast-like cell. An A-V loop can make the scaffold axially vascularized, which may be used for microsurgical graft transfer at a defect site. The FG hydrogel was degraded quickly with fast generation of supporting tissue, which seems attractive to apply with cells that require quick supply of nutrition. On the contrary, hyaluronan hydrogel was gradually degraded that guided slow and sustained growth of blood vessels and FVT. On this basis, it can be concluded that the PLDLLA-TCP-PCL-hydrogel scaffolds can possibly be explored for vascularized bone engineering application.

Acknowledgements

This study was supported by Deutsche Forschungsgemeinschaft (DFG) research grant KN 578/2-1. The authors thank Kim Ching from Temasek Polytechnic, Singapore for helping in the scaffold fabrication. The authors gratefully acknowledge the help of Dr Galyna Pryymachuk in microsurgical procedures for *in vivo* experiments. The authors thank Dr Andreas Hess, Institute of Experimental and Clinical Pharmacology and Toxicology for helping in micro-CT scanning and Prof. Peter Greil and Mr Peter Reinhard for production of the Teflon chambers.

References

1. Arkudas A, Tjiawi J, Bleiziffer O, Grabinger L, Polykandriotis E, Beier JP, et al. Fibrin gel-immobilized VEGF and bFGF efficiently stimulate angiogenesis in the AV loop model. *Mol Med* 2007; 13: 480–487.
2. Folkman JH and Hochberg M. Self regulation of growth in three dimensions. *J Exp Med* 1973; 138: 745–753.
3. Hutmacher DW, Horch RE, Loessner D, Rizzi S, Sieh S, Reichert JC, et al. Translating tissue engineering technology platforms into cancer research. *J Cell Mol Med* 2009; 13: 1417–1427.
4. Steffens L, Wenger A, Stark G and Finkenzeller G. In vivo engineering of a human vasculature for bone tissue engineering applications. *J Cell Mol Med* 2009; 13: 3380–3386.
5. Kneser U, Schaefer DJ, Polykandriotis E and Horch RE. Tissue engineering of bone: the reconstructive surgeon's point of view. *J Cell Mol Med* 2006; 10: 7–19.
6. Lokmic Z, Stillaert F, Morrison WA, Thompson EW and Mitchell GM. An arteriovenous loop in a protected space generates a permanent, highly vascular, tissue-engineered construct. *FASEB J* 2007; 21: 511–522.
7. Tanaka Y, Sung KC, Tsutsumi A, Ohba S, Ueda K and Morrison WA. Tissue engineering skin flaps: which vascular carrier, arteriovenous shunt loop or arteriovenous bundle, has more potential for angiogenesis and tissue generation? *Plast Reconstr Surg* 2003; 112: 1636–1644.
8. Polykandriotis E, Euler S, Arkudas A, Pryymachuk G, Beier JP, Greil P, et al. Regression and persistence: remodelling in a tissue engineered axial vascular assembly. *J Cell Mol Med* 2009; 13: 4166–4175.
9. Sung H, Meredith C, Johnson C and Galis Z. The effect of scaffold degradation rate on three-dimensional cell growth and angiogenesis. *Biomaterials* 2004; 25: 5735–5742.
10. Rezwan K, Chen Q, Blaker J and Boccaccini A. Biodegradable and bioactive porous polymer/inorganic composite scaffolds for bone tissue engineering. *Biomaterials* 2006; 27: 3413–3431.
11. Schmidmaier G, Wildemann B, Bail H, Lucke M, Fuchs T, Stemberger A, et al. Local application of growth factors (insulin-like growth factor-1 and transforming growth factor-ß1) from a biodegradable poly (d, l-lactide) coating of osteosynthetic implants accelerates fracture healing in rats. *Bone* 2001; 28: 341–350.
12. Hutmacher DW. Scaffolds in tissue engineering bone and cartilage. *Biomaterials* 2000; 21: 2529–2543.
13. Shor L, Güçeri S, Chang R, Gordon J, Kang Q, Hartsock L, et al. Precision extruding deposition (PED) fabrication of polycaprolactone (PCL) scaffolds for bone tissue engineering. *Biofabrication* 2009; 1: 015003.
14. Heidemann W, Jeschkeit S, Ruffieux K, Fischer J, Wagner M, Krüger G, et al. Degradation of poly (d, l) lactide implants with or without addition of calciumphosphates in vivo. *Biomaterials* 2001; 22: 2371–2381.
15. Endres M, Hutmacher DW, Salgado AJ, Kaps C, Ringe J, Reis RL, et al. Osteogenic induction of human bone marrow-derived mesenchymal progenitor cells in novel synthetic polymer-hydrogel matrices. *Tissue Eng* 2003; 9: 689–702.
16. Ferreira L, Gerecht S, Fuller J, Shieh H, Vunjak-Novakovic G and Langer R. Bioactive hydrogel scaffolds for controllable vascular differentiation of human embryonic stem cells. *Biomaterials* 2007; 28: 2706–2717.
17. Hoffman A. Hydrogels for biomedical applications. *Adv Drug Deliv Rev* 2002; 54: 3–12.
18. Hong L, Tabata Y, Miyamoto S, Yamamoto M, Yamada K, Hashimoto N, et al. Bone regeneration at rabbit skull defects treated with transforming growth factor-beta 1 incorporated into hydrogels with different levels of biodegradability. *J Neurosurg* 2000; 92: 315–325.
19. Arnander C, Westermark A, Veltheim R, Docherty-Skogh AC, Hilborn J and Engstrand T. Three-dimensional technology and bone morphogenetic protein in frontal bone reconstruction. *J Craniofac Surg* 2006; 17: 275–279.
20. Toole BP and Hascall VC. Hyaluronan and tumor growth. *Am J Pathol* 2002; 161: 745–747.
21. Shu XZ, Liu Y, Palumbo FS and Luo Y. In situ crosslinkable hyaluronan hydrogels for tissue engineering. *Biomaterials* 2004; 25: 1339–1348.
22. Lam C, Olkowski R, Swieszkowski W, Tan K, Gibson I and Hutmacher D. Mechanical and in vitro evaluations of composite PLDLLA/TCP scaffolds for bone engineering. *Virtual Phys Prototyping* 2008; 3: 193–197.
23. Kneser U, Polykandriotis E, Ohnolz J, Heidner K, Grabinger L, Euler S, et al. Engineering of vascularized transplantable bone tissues: induction of axial vascularization in an osteoconductive matrix using an arteriovenous loop. *Tissue Eng* 2006; 12: 1721–1731.
24. Polykandriotis E, Arkudas A, Beier JP, Hess A, Greil P, Papadopoulos T, et al. Intrinsic axial vascularization of an osteoconductive bone matrix by means of an arteriovenous vascular bundle. *Plast Reconstr Surg* 2007; 120: 855–868.
25. Arkudas A, Pryymachuk G, Hoereth T, Beier J, Polykandriotis E, Bleiziffer O, et al. Dose-finding study of fibrin gel-immobilized vascular endothelial growth factor 165 and basic fibroblast growth factor in the arteriovenous loop rat model. *Tissue Eng Pt A* 2009; 15: 2501–2511.
26. Athanasiou KA, Zhu C, Lanctot DR, Agrawal CM and Wang X. Fundamentals of biomechanics in tissue engineering of bone. *Tissue Eng* 2000; 6: 361–381.
27. Slivka MA, Leatherbury NC, Kieswetter K and Niederauer GG. Porous, resorbable, fiber-reinforced scaffolds tailored for articular cartilage repair. *Tissue Eng* 2001; 7: 767–780.
28. Karageorgiou V and Kaplan D. Porosity of 3D biomaterial scaffolds and osteogenesis. *Biomaterials* 2005; 26: 5474–5491.
29. Temenoff J, Park H, Jabbari E, Conway D, Sheffield T, Ambrose C, et al. Thermally cross-linked oligo (poly (ethylene glycol) fumarate) hydrogels support osteogenic differentiation of encapsulated marrow stromal cells in vitro. *Biomacromolecules* 2004; 5: 5–10.

30. Smith JD, Chen A, Ernst LA, Waggoner AS and Campbell PG. Immobilization of aprotinin to fibrinogen as a novel method for controlling degradation of fibrin gels. *Bioconjugate Chem* 2007; 18: 695–701.
31. Vanderhooft JL, Mann BK and Prestwich GD. Synthesis and characterization of novel thiol-reactive poly(ethylene glycol) cross-linkers for extracellular-matrix-mimetic. *Biomacromolecules* 2007; 8: 2883–2889.
32. Peled E, Boss J, Bejar J, Zinman C and Seliktar D. A novel poly (ethylene glycol)-fibrinogen hydrogel for tibial segmental defect repair in a rat model. *J Biomed Mater Res A* 2007; 80: 874–884.
33. Le Nihouannen D, Guehennec LL, Rouillon T, Pilet P, Bilban M, Layrolle P, et al. Micro-architecture of calcium phosphate granules and fibrin glue composites for bone tissue engineering. *Biomaterials* 2006; 27: 2716–2722.
34. Schliephake H, Weich H, Dullin C, Gruber R and Frahse S. Mandibular bone repair by implantation of rhBMP-2 in a slow release carrier of polylactic acid–An experimental study in rats. *Biomaterials* 2008; 29: 103–110.
35. Riley CM, Fuegy PW, Firpo MA, Shu XZ, Prestwich GD and Peattie RA. Stimulation of in vivo angiogenesis using dual growth factor-loaded crosslinked glycosaminoglycan hydrogels. *Biomaterials* 2006; 27: 5935–5943.
36. Terheyden H, Menzel C, Wang H, Springer IN, Rueger DR and Acil Y. Prefabrication of vascularized bone grafts using recombinant human osteogenic protein-1–part 3: dosage of rhOP-1, the use of external and internal scaffolds. *Int J Oral Maxillofac Surg* 2004; 33: 164–172.